Reprinted from JOURNAL OF APPLIED METEOROLOGY, Vol. 19, No. 6, June 1980
American Meteorological Society

Spectral Variation of Optical Depth at Tucson, Arizona between August 1975 and December 1977

MICHAEL D. KING[1]

Laboratory for Atmospheric Sciences, Goddard Space Flight Center, NASA, Greenbelt, MD 20771

DALE M. BYRNE[1]

United Technologies Research Center, West Palm Beach, FL 33402

JOHN A. REAGAN AND BENJAMIN M. HERMAN

The University of Arizona, Tucson 85721

(Manuscript received 10 December 1979, in final form 20 March 1980)

ABSTRACT

A multi-wavelength solar radiometer has been used to monitor the directly transmitted solar radiation at discrete wavelengths spaced through the visible and near-infrared wavelength regions. The relative irradiance of the directly transmitted sunlight at each wavelength was measured during the course of each cloud-free day, from which the total optical depth of the atmosphere was determined using the Bouguer-Langley method. From the spectral variation of total optical depth the ozone absorption optical depths, and hence total ozone content of the atmosphere, have been derived. By subtracting the molecular scattering and estimated ozone absorption contributions from the total optical depth, the aerosol optical depth for each day and wavelength can be determined provided the wavelengths selected have no additional molecular absorption bands. Results of this analysis for 133 clear stable days at Tucson, Arizona are presented for a 29-month period between August 1975 and December 1977. Monthly averages of the total and aerosol optical depths are presented for five wavelengths between 0.4400 and 0.8717 μm. The aerosol optical depth obtains a maximum in July and August with a secondary maximum in April and May. The median aerosol optical depth for the entire data set decreases with wavelength from 0.0508 (λ = 0.4400 μm) to 0.0306 (λ = 0.8717 μm). Also presented are daily values of total ozone content which exhibit the characteristic seasonal cycle with peak values in early May and an annual mean value of 275 m atm-cm.

1. Introduction

The optical thickness of the atmosphere is an important parameter affecting the transfer of radiant energy in the earth's atmosphere. The optical thickness of the cloud-free atmosphere depends to a large extent on the variable amount of ozone, water vapor and aerosol particles, the effects of which may be strongly wavelength dependent. By measuring the relative irradiance of the directly transmitted sunlight at selected wavelengths during the course of a cloud-free day, it is possible to determine not only the aerosol optical depth and total ozone content (King and Byrne, 1976; Shaw, 1979b) but also an estimate of the aerosol size distribution (King *et al.*, 1978).

Flowers *et al.* (1969) presented the results of a relatively long period of observations (1961–66) of the aerosol optical thickness for a single wavelength interval centered at 0.50 μm as determined using a Volz sunphotometer. The unique feature of this study was the comparison of turbidity measurements from 29 different stations within the United States with all measurements being made with the same type of instrument and using the same analysis techniques. Their results show very clearly the large differences in turbidity which occur as a function of time of year and locality.

More information concerning the properties of aerosol particles is contained in measurements of the wavelength dependence of the optical depth as first suggested by Ångström (1929). Atmospheric transmission measurements at two wavelengths have often been collected at individual stations in order to estimate the parameters of Ångström's (1929) empirical formula for the wavelength dependence of the aerosol optical thickness. Among the more recent studies of this kind are measurements in Poona, India (Rangarajan, 1972), Page, Arizona (Malm *et al.*, 1977; Malm and Walther, 1979), and the Los Angeles Basin (Peterson *et al.*, 1978a,b).

[1] These authors were at the University of Arizona, Tucson, when the measurements described herein were taken.

0021-8952/80/060723-10$06.50

These studies have ranged between spatial distribution studies for a 2-day period (Peterson *et al.*, 1978a) to studies at a single station for periods of a year or longer (Rangarajan, 1972; Malm *et al.*, 1977; Malm and Walther, 1979).

Yamamoto and Tanaka (1969), Quenzel (1970) and King *et al.* (1978) have demonstrated that parameters of an aerosol size distribution can be inferred from aerosol optical depth (or volume extinction coefficient) measurements at several wavelengths. In addition to these studies, multi-wavelength aerosol optical depth measurements have been presented and discussed by Shaw *et al.* (1973), Roosen *et al.* (1973), Fraser (1975), King and Byrne (1976), Carlson and Caverly (1977) and Shaw (1979a). Each of these studies included measurements in at least seven spectral intervals from the near-ultraviolet to the near-infrared. Only the study by Roosen *et al.* (1973) contained results from many different sites (13) at many different wavelengths (10) over a long period of time (~50 years). This was a consequence of using the data base obtained by the Astrophysical Observatory of the Smithsonian Institution as part of their solar constant monitoring program.

The accuracy of the determination of the aerosol optical depth depends on the wavelengths and bandwidth intervals selected for the measurements. If the total optical depth is measured at wavelengths excluding the strong selective absorption bands of the atmosphere, an important uncertainty in determining the aerosol optical depth still remains. This uncertainty is associated with the variable amount of ozone in the atmosphere. Until recently, it was customary when analyzing spectral optical depth measurements to either assume a constant value for total ozone content (e.g., Flowers *et al.*, 1969; Rangarajan, 1972) or to assume a seasonal cycle for the appropriate latitude of the measurements (e.g., Shaw *et al.*, 1973).

In the present study an earlier technique (King and Byrne, 1976) for inferring the daily value of the total ozone content of the atmosphere has been applied to spectral optical depth measurements obtained at Tucson for a 29-month period between August 1975 and December 1977. After discussing the selection of wavelength regions appropriate for aerosol optical depth determinations in the visible and near-infrared, monthly averages of the total and aerosol optical depths are presented for five wavelengths between 0.4400 and 0.8717 μm. Finally, daily values of total ozone content are presented for the entire 133-day data set.

2. Determination of total and aerosol optical depths

The relative irradiance of the directly transmitted solar radiation was measured during the course of each cloud-free day with a multi-wavelength solar radiometer described by Shaw *et al.* (1973). Data are presented here which have been collected in Tucson between August 1975 and December 1977. During this period five of the eight filters whose wavelengths were centered at 0.4400, 0.5217, 0.6120, 0.7797 and 0.8717 μm were in continuous use; thus optical depth results will be presented for these wavelengths only. For all of these filters the full bandwidth at half-peak transmittance was less than or equal to 0.0120 μm.

Shaw (1976) has discussed the error terms involved in precision sun photometry. These error terms include instrumental errors, calibration errors and errors imposed by the atmosphere. Based on that study it can be concluded that uncertainties brought about by diffuse radiation within the field of view of the radiometer, in this case 3°, are negligible for the wavelengths and aerosol optical depths presented below. The total optical depth of the atmosphere was determined for each cloud-free day, or portion of a day, by making a fit to the Lambert-Beer law given by

$$F(\lambda) = F_0(\lambda) \exp[-\tau_t(\lambda) m(\theta_0)], \quad (1)$$

where $F(\lambda)$ is the solar irradiance reaching the detector at wavelength λ; $F_0(\lambda)$ the irradiance incident on the top of the atmosphere; $m(\theta_0)$ the atmospheric air mass, a function of solar zenith angle θ_0; and $\tau_t(\lambda)$ the total optical depth.

In the absence of an instrumental calibration of the extraterrestrial solar irradiance, it is customary to determine $\tau_t(\lambda)$ by making a linear least-squares fit to $\ln F(\lambda)$ as a function of $m(\theta_0)$, with the resulting slope being the negative of the total optical depth. This method, known as the Bouguer-Langley method, has been discussed and applied by many investigators (e.g., Shaw *et al.*, 1973; Fraser, 1975; King and Byrne, 1976; Shaw, 1979a) and will not be repeated here. The reader is referred to King and Byrne (1976) for a more complete discussion of the method, including an example of a Langley plot [$\ln F(\lambda)$ vs $m(\theta_0)$] and the empirical expression for airmass used in this investigation (after Rozenberg, 1966).

It is well known that temporal and spatial fluctuations in the atmosphere can lead to nonlinear Langley plots and hence invalidate the method for a particular day. In these instances no analysis has been pursued since a single optical depth value does not characterize the atmospheric transmission for a large portion of a day. Peterson *et al.* (1978b) and Shaw (1979a) have observed atmospheric transmission from mountain stations for which it is common to have stable and nearly constant values of the optical depth in the morning with temporal fluctuations in the afternoon. These afternoon fluctuations are due to temperature inversions below the station which dissipate in mid to late morning, followed by convection of low-level aerosol particles over the mountain stations. Tucson, on the other hand, is in a

valley surrounded by mountains and it is more common to have stable optical depths in the afternoon with changing conditions in the morning. During the morning hours the relative humidity is initially large and radiative temperature inversions are common. It is not until mid or late morning that the temperature inversion dissipates and the humidity decreases. Many of the optical depth results presented below thus apply to afternoon conditions, although some of the results are based on observations over the entire day.

As pointed out by Golovachev *et al.* (1972), Russell and Shaw (1975) and Shaw (1976), the linearity of a Langley plot does not necessarily guarantee that temporal fluctuations in $\tau_t(\lambda)$ do not occur. Under these conditions, however, an intercept value of $F_0(\lambda)$ would be inferred which is in error and different from the intercept values determined independently from preceding or subsequent days. The data presented below have been selected according to the linearity of the Langley plots and the consistency of the estimated intercept values of $F_0(\lambda)$. In most instances the uncertainty of the total optical depth was 0.0020 or less although occasionally uncertainties as large as 0.0040 occurred. The uncertainty of the intercept value was typically 1% of $F_0(\lambda)$, with slightly larger uncertainties at the shorter wavelengths ($\lambda \leq 0.5217$ μm) and slightly smaller uncertainties at the longer wavelengths ($\lambda \geq 0.6120$ μm). Since the solar radiometer was not calibrated, this uncertainty in the intercept voltage level, which is proportional to $F_0(\lambda)$, does not imply an absolute determination of the extraterrestrial solar irradiance to this accuracy.

Once the total optical depths have been determined, one can determine corresponding values of the aerosol optical depth τ_a by subtracting from τ_t the contribution due to molecular scattering τ_R, known as the Rayleigh optical depth, and the contribution of the ozone Chappuis absorption band τ_{O_3}, known as the ozone optical depth. Further corrections to the total optical depth may be necessary if the wavelengths have been selected in bands of strong selective absorption by atmospheric gases, such as water vapor or oxygen. The gaseous absorption features in the visible and near-infrared wavelength regions are discussed in the next section. In the absence of additional molecular absorption it therefore follows that

$$\tau_a(\lambda,p,\eta) = \tau_t(\lambda) - \tau_R(\lambda,p) - \eta a(\lambda), \qquad (2)$$

where $\tau_R(\lambda,p)$ is the spectral value of the Rayleigh optical depth, a function of surface pressure p; $a(\lambda)$ the ozone absorption coefficient per centimeter of pure gas at STP; and η the total ozone content of the atmosphere measured in atm-cm.[2]

[2] 1 atm-cm = 2.687×10^{19} molecules cm^{-2} in a vertical column.

Since the pressure is relatively constant from day to day and easily measured with a barometer, it is relatively simple to compute the Rayleigh optical thickness after assuming a value for the molecular depolarization factor, in this case 0.035. Although there have been recent suggestions that this value may be slightly too large (e.g., Gucker *et al.*, 1969; Hoyt, 1977), the resulting uncertainty is small compared to other uncertainties. The largest systematic errors in determining the aerosol optical depths at wavelengths in the mid-visible region are associated with uncertainties in the values of the ozone optical depths. This problem has been discussed in detail by King and Byrne (1976) who described a procedure whereby the O_3 absorption optical depths, and hence total ozone content of the atmosphere, could be inferred from the spectral variation of total optical depth in the visible and near-infrared wavelength regions. The basis of this technique was the observation that $\log\tau_a$ is very nearly a linear function of $\log\lambda$ for a wide variety of aerosol size distributions. As a result, the observations of $\log\tau_a(\lambda,p,\eta)$ calculated from (2) were fitted to a quadratic of the form

$$\log\hat{\tau}_a = b_0 + b_1 \log\lambda + b_2(\log\lambda)^2 \qquad (3)$$

in order to determine the total ozone content η and the coefficients b_0, b_1 and b_2. The inclusion of the quadratic term enables more realistic fits to non-Junge aerosol size distributions as well as to Junge distributions extending over finite radii limits.

Maximizing the probability that the $\log\tau_a(\lambda,p,\eta)$ observations have the functional form of (3) is equivalent to minimizing the statistic χ^2 defined as

$$\chi^2 = \sum_i \frac{1}{\sigma'^2}[\log\tau_a(\lambda_i,p,\eta) - \log\hat{\tau}_a]^2$$

$$= \sum_i \frac{1}{\sigma'^2}[\log\tau_a(\lambda_i,p,\eta) - b_0 - b_1\log\lambda_i - b_2(\log\lambda_i)^2]^2, \qquad (4)$$

where the summation extends over all λ_i for which no additional molecular absorption occurs and σ_i' represents the standard deviations of the $\log\tau_a(\lambda_i,p,\eta)$ values. The weighting factors σ_i' appropriate to the logarithmic scale can be calculated by the method of propagation of errors (see, e.g., Bevington, 1969). In this instance $\sigma_i'^2$ can be written as (King and Byrne, 1976)

$$\sigma_i'^2 = \sigma_i^2\left[\frac{\log e}{\tau_a(\lambda_i,p,\eta)}\right]^2, \qquad (5)$$

where σ_i represents the uncertainty in $\tau_a(\lambda_i)$.

Minimizing χ^2 as defined by (4) is equivalent to making a weighted least-squares fit to the data. Once the value of η at which χ^2 attains a minimum is found, this value of η is multiplied by the ozone absorption coefficients at the several wavelengths to

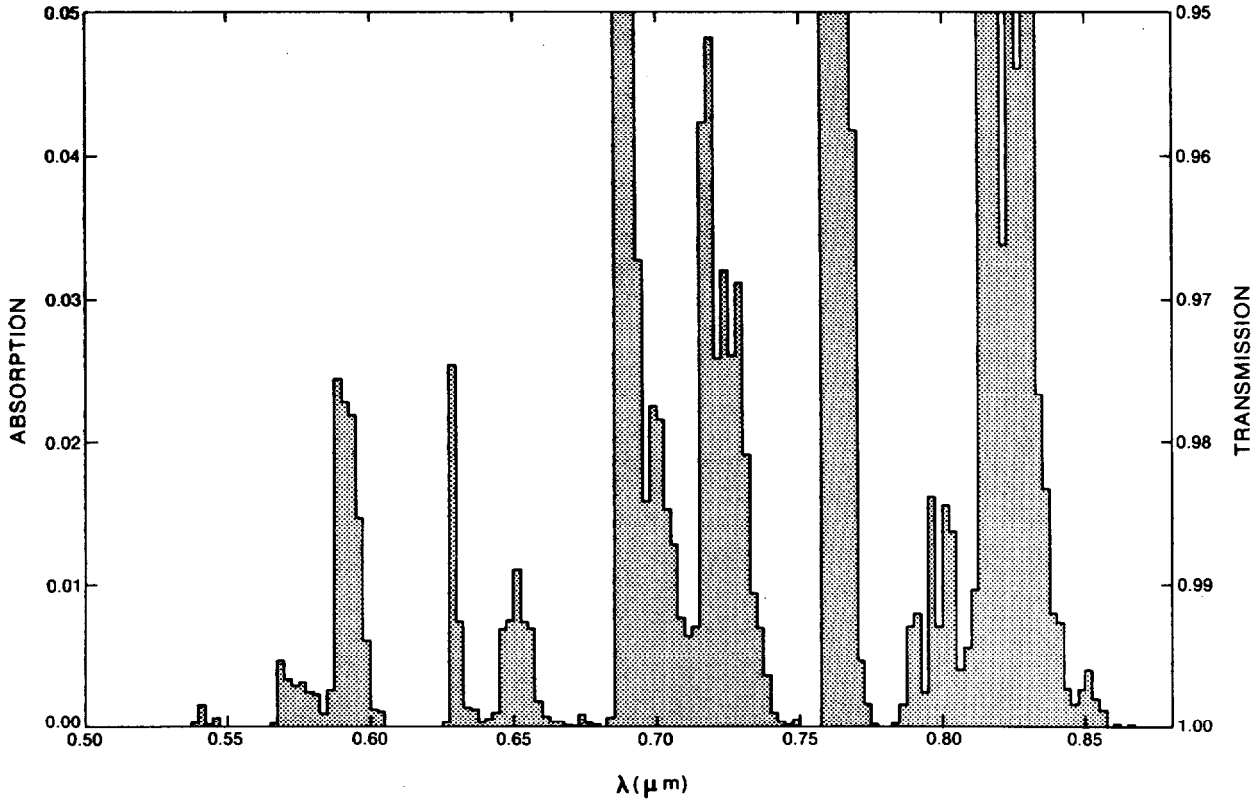

FIG. 1. Slant path absorption and transmission through the atmosphere (at a resolution of 25 Å) as obtained from high resolution spectra in the *Utrecht Photometric Atlas* (after Moore *et al.*, 1966). Bands at 0.63, 0.69 and 0.76 μm are due to oxygen absorption while all remaining bands are due to water vapor absorption. The air mass varies with wavelength but is everywhere less than 2.22 (see text for details).

obtain the optimum spectral correction. The complete details of this procedure, including the formulas for obtaining standard deviation estimates of η, may be found in King and Byrne (1976). A simple variation of this method was recently used by Shaw (1979b) to compare total ozone contents thus obtained with those determined simultaneously with a Dobson ozone spectrophotometer. The O_3 absorption coefficients used in the present investigation were those tabulated by Ackerman (1971). These represent a composite of measurement results reported by other observers. A summary of results for the total ozone contents as well as the total and aerosol optical depths are presented and discussed in Section 4.

3. Selection of wavelengths

In selecting the wavelengths for making direct solar transmission measurements, it is often advantageous to choose wavelength regions at appropriate positions and of appropriate widths to avoid the bands of strong selective absorption by the atmosphere. In the visible and near-infrared wavelength regions the atmospheric gases which produce strong rotation-vibration absorption bands are water vapor and oxygen. In addition to these bands, there is a relatively strong ozone continuum extending from approximately 0.4–0.9 μm with a maximum located near 0.6 μm. Due to the broad extent of this absorption band, known as the Chappuis continuum, it is not possible to avoid O_3 absorption when making solar transmission measurements in the visible wavelength region, but approximate corrections for O_3 can easily be made as discussed in the preceding section. Nitrogen dioxide also has a continuum absorption band extending from approximately 0.34–0.50 μm with a maximum located near 0.41 μm (cf. Chu and McCormick, 1979). Its magnitude is sufficiently small such that it is relatively unimportant for surface based optical thickness measurements.

Except for the continuum absorption bands of NO_2 and O_3, the terrestrial absorption lines appear only for $\lambda > 0.54$ μm (Moore *et al.*, 1966). Fig. 1 illustrates the positions and magnitudes of the atmospheric bands from 0.50 to 0.88 μm which have been obtained from the compendium of solar spectrum wavelengths, measured equivalent widths and absorption line identifications presented by Moore *et al.* (1966). The resolution presented here (*viz.*, 25 Å) is too large to resolve the individual absorp-

tion lines but adequate for delineating the many different absorption bands. The absorption bands near 0.63, 0.69 and 0.76 μm are due to O_2 absorption (α, B and A bands, respectively) while all remaining absorption bands are due to H_2O.

The equivalent widths reported by Moore *et al.* (1966) were obtained by measuring the spectra in the *Utrecht Photometric Atlas* (Minnaert *et al.*, 1940). Because of the time needed to perform the measurements, the atmospheric airmass varies with wavelength. All the results presented in Fig. 1 were obtained from the Mount Wilson Observatory when the airmass $m(\theta_0) \leq 2.22$. Recent measurements by Koepke and Quenzel (1978) of atmospheric transmission near three water vapor bands (0.72, 0.82 and 0.93 μm) indicate absorption curves of similar shape as those in Fig. 1 but of larger magnitude. This is due to either a larger water vapor content or larger airmass in Koepke and Quenzel's (1978) results than in those at the time of Minnaert *et al.*'s (1940) measurements.

For aerosol optical thickness determinations, it is preferable to select wavelength intervals which avoid these absorption features than to try to overlap the bands and make corrections for additional molecular absorption. Based on the results presented in Fig. 1 for $\lambda < 0.88$ μm and those of McClatchey *et al.*[3] for $\lambda > 0.88$ μm, Table 1 has been constructed. This table summarizes all of the wavelength regions from the near-ultraviolet to the near-infrared where absorption by water vapor and oxygen can be neglected. The five wavelengths for which measurement results are presented below have been selected with Table 1 in mind. Additional wavelengths which have been used between August 1975 and December 1977 are 0.3714, 0.5556, 0.6708, 0.6893, 0.7120 and 1.0303 μm. Only in the case of 0.6893 and 0.7120 μm were additional molecular absorption corrections required. These can be made by methods described by King and Byrne (1976).

4. Results

The method for inferring total ozone content and aerosol optical depths described in Section 2 has been carried out at the University of Arizona (latitude 32°14′) since August 1975. Between August 1975 and December 1977, 133 days of data were selected as previously described. Since days with large temporal fluctuations in the optical depth have been eliminated from the analysis, it follows that the results presented below represent a somewhat biased data set to the extent that some of the days with largest turbidities, days for which large temporal fluctuations are common, have not been included. The aerosol optical depth data for each of the five wavelengths (0.4400, 0.5217, 0.6120, 0.7797 and 0.8717 μm) were sorted according to the magnitude of τ_a in order to obtain a cumulative distribution of τ_a at each wavelength. Fig. 2 illustrates the percentage of days at each wavelength for which the aerosol optical depths were below the magnitudes indicated. The 50% curve, which represents the median values of τ_a, decreases with wavelength

TABLE 1. Wavelength regions from the near-ultraviolet to the near-infrared where molecular absorption can be neglected [after Moore *et al.* (1966) for $\lambda < 0.88$ μm and McClatchey *et al.*[3] for $\lambda > 0.88$ μm].

Wavelength range (μm)	Comments
0.3550–0.5390	Completely clear
0.5480–0.5665	Completely clear
0.6050–0.6265	Completely clear
0.6590–0.6865	Clear with average absorption of 0.03%
0.7400–0.7590	Clear with average absorption of 0.03%
0.7740–0.7860	Clear with average absorption of 0.01%
0.8575–0.8770	Clear with average absorption of 0.01%
1.0200–1.0450	Clear

Note: The NO_2 and O_3 continuums are not included.

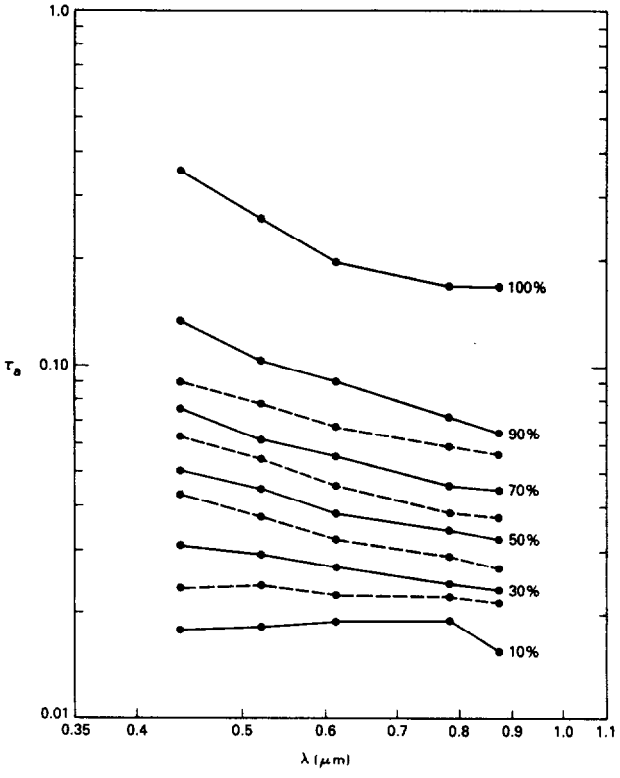

FIG. 2. Percentage of days at each wavelength for which the aerosol optical depths were below the magnitudes indicated. The 50% curve thus represents the median values of τ_a for the entire 133 observation-day, 29-month record.

[3] McClatchey, R. A., R. W. Fenn, J. E. A. Selby, F. E. Volz and J. S. Garing, 1972: Optical properties of the atmosphere, 3rd ed. Rep. AFCRL-72-0497, Air Force Cambridge Research Laboratories, 108 pp. [NTIS AD753075].

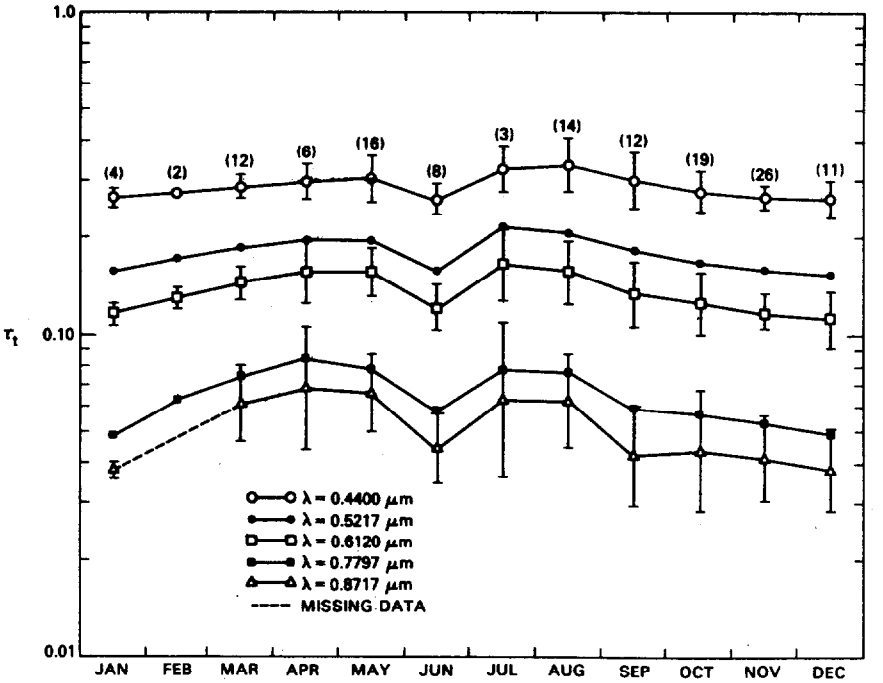

FIG. 3. Geometric mean values of total optical depth by month at five wavelengths. The numbers in parentheses indicate the total number of days involved in the average. Logarithmic standard deviations of the total optical depth are included for three wavelengths.

from 0.0508 (λ = 0.4400 μm) to 0.0306 (λ = 0.8717 μm). The 100% curve represents the largest magnitudes of τ_a obtained over the 29-month record. Those at the shortest wavelengths ($\lambda \leq 0.6120$ μm) were obtained on 7 August 1975, a day for which the aerosol optical depth measurements very nearly follow Ångström's (1929) empirical formula given by $\tau_a(\lambda) = \beta\lambda^{-\alpha}$ [see Fig. 2 of King *et al.* (1978) for an illustration of the spectral optical depth data and inverted aerosol size distribution for this day]. The maximum τ_a data at the longest wavelengths ($\lambda \geq 0.7797$ μm) were obtained on 23 October 1975, a day for which there was a dust storm event with little wavelength dependence of τ_a [see Fig. 5 of King and Byrne (1976) for an illustration of the spectral optical depth data for this day].

In Fig. 2, as well as in the data for most of the individual days, the largest turbidities (aerosol optical depths) were associated with large values of the Ångström turbidity coefficient (α) while low turbidities were associated with low values of α. This was discussed previously for the Tucson data by King *et al.* (1978) where the implications for the aerosol size distributions were emphasized. This trend has also been observed in the Los Angeles Basin (Peterson *et al.*, 1978a,b), Page, Arizona (Malm *et al.*, 1977), Poona, India (Rangarajan, 1972) and Mauna Loa Observatory (Shaw, 1979a). Only in the cases of wind raised dust of large particle sizes are high turbidities characterized by small values of α. These cases are occasionally observed in Tucson (e.g., 23 October 1975 as mentioned above) but are found to be quite common in the GATE area of the tropical Atlantic (Carlson and Caverly, 1977).

The minimum aerosol optical depth for each wavelength, which would correspond to the 0% level in Fig. 2 (not shown), is slightly below τ_a = 0.01 for all wavelengths. Careful inspection of Fig. 2 suggests that the probability distribution of τ_a values is nearly symmetric about the median level. Since the ordinate scale in Fig. 2 is $\log\tau_a$, rather than τ_a, it implies that the aerosol optical depth is more nearly log-normally distributed than normally distributed, as also suggested by Malm *et al.* (1977). To test this hypothesis the arithmetic mean and standard deviation, as well as the geometric mean and logarithmic standard deviation, of τ_a for each wavelength were computed. The arithmetic mean was always larger than the median and corresponded to the 62% level of the cumulative distribution with the percentage of days within one standard deviation of the mean accounting for 81% of the population. The geometric mean values of τ_a were always near the median values with the average for all wavelengths being at the 49% level of the cumulative distribution. The percentage of days within one logarithmic standard deviation of the geometric mean was 72%, which is near the normal distribution value of 68%. As a consequence, geometric rather than arithmetic means have been used in subsequent analysis.

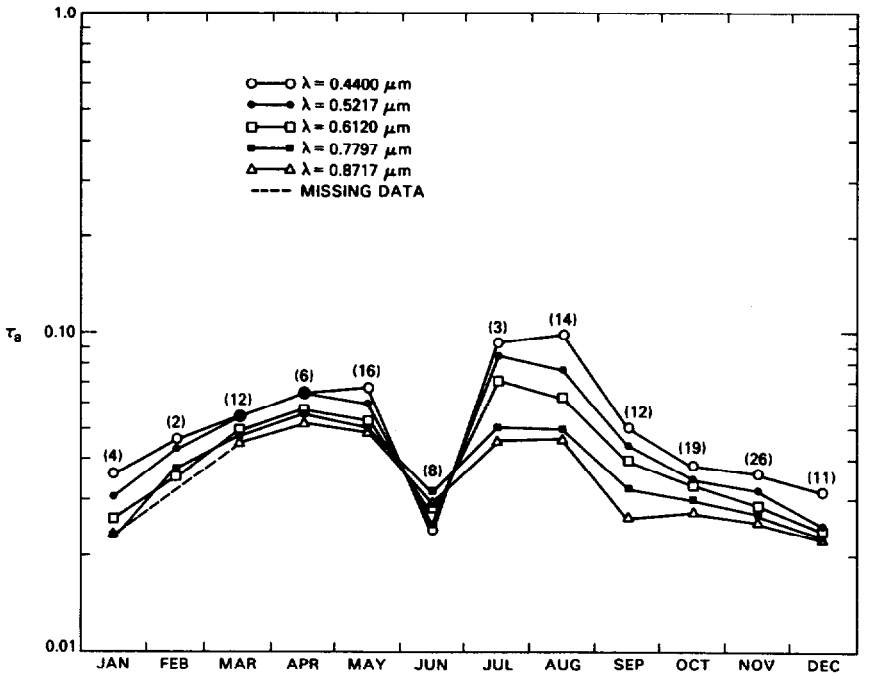

FIG. 4. Geometric mean values of aerosol optical depth by month at five wavelengths. The numbers in parentheses indicate the total number of days involved in the average.

Fig. 3 shows the monthly variation of the geometric mean values of total optical depth at each of the five wavelengths. The number of days contributing to each monthly average is indicated by the numbers in parentheses. The error bars in the figure represent the limits of one logarithmic standard deviation of τ_t, which is equivalent to one standard deviation of $\log\tau_t$. The error bars are illustrated for only three wavelengths in order to avoid overlap. Since the total optical depth includes Rayleigh scattering, the curves for the individual wavelengths are distinctly separated. The results for the aerosol optical depths show less wavelength dependence than the total optical depths, as seen upon examination of Fig. 4. The geometric mean aerosol optical depths ($\bar{\tau}_a$) and logarithmic standard deviations of the aerosol optical depths (σ_a) are presented in Table 2 for each of the five wavelengths.

Examination of Fig. 4 suggests that the aerosol optical depth obtains a maximum in July and August with a secondary maximum in April and May. The minimum values of τ_a obtained in June and in December and January are also apparent from Figs. 3 and 4. In late May and June the winds over much of Arizona are from the west and the air is hot and dry, thus inhibiting cloud and rainstorm development.

TABLE 2. Summary of the monthly mean Ångström turbidity coefficient, geometric mean aerosol optical depth and logarithmic standard deviation of the aerosol optical depth for Tucson, Arizona between August 1975 and December 1977.

Month	Number of days	α	λ = 0.4400 μm		λ = 0.5217 μm		λ = 0.6120 μm		λ = 0.7797 μm		λ = 0.8717 μm	
			$\bar{\tau}_a$	σ_a	$\bar{\tau}_a$	σ_a	$\bar{\tau}_a$	σ_a	$\bar{\tau}_a$	σ_a	$\bar{\tau}_a$	σ_a
January	4	0.46 ± 0.64	0.0360	0.2323	0.0305	0.1551	0.0261	0.1277	0.0233	0.0611	0.0233	0.0475
February	2	0.62 ± 0.08	0.0461	0.0472	0.0434	0.0749	0.0357	0.0395	0.0376	0.0652		
March	12	0.23 ± 0.67	0.0550	0.2316	0.0547	0.1901	0.0494	0.1698	0.0478	0.1347	0.0457	0.1505
April	6	0.12 ± 0.36	0.0645	0.2946	0.0649	0.2497	0.0570	0.2804	0.0564	0.2443	0.0520	0.2576
May	16	0.43 ± 0.70	0.0674	0.3039	0.0600	0.2496	0.0535	0.2187	0.0504	0.1753	0.0503	0.1579
June	8	−0.16 ± 0.84	0.0242	0.4948	0.0250	0.4617	0.0281	0.3198	0.0314	0.2091	0.0289	0.1636
July	3	1.04 ± 0.22	0.0934	0.2718	0.0845	0.2213	0.0710	0.2232	0.0505	0.2889	0.0458	0.3383
August	14	1.07 ± 0.69	0.0987	0.2731	0.0767	0.2358	0.0628	0.2210	0.0499	0.2022	0.0467	0.1920
September	12	0.91 ± 1.01	0.0504	0.5321	0.0441	0.4355	0.0397	0.3394	0.0325	0.2447	0.0262	0.2506
October	19	0.40 ± 0.97	0.0385	0.3950	0.0340	0.4097	0.0332	0.3231	0.0300	0.2659	0.0273	0.2740
November	26	0.42 ± 0.44	0.0360	0.2638	0.0320	0.2266	0.0289	0.2052	0.0270	0.1975	0.0255	0.2154
December	11	0.16 ± 0.50	0.0316	0.2910	0.0246	0.3039	0.0239	0.2725	0.0229	0.2309	0.0228	0.2070

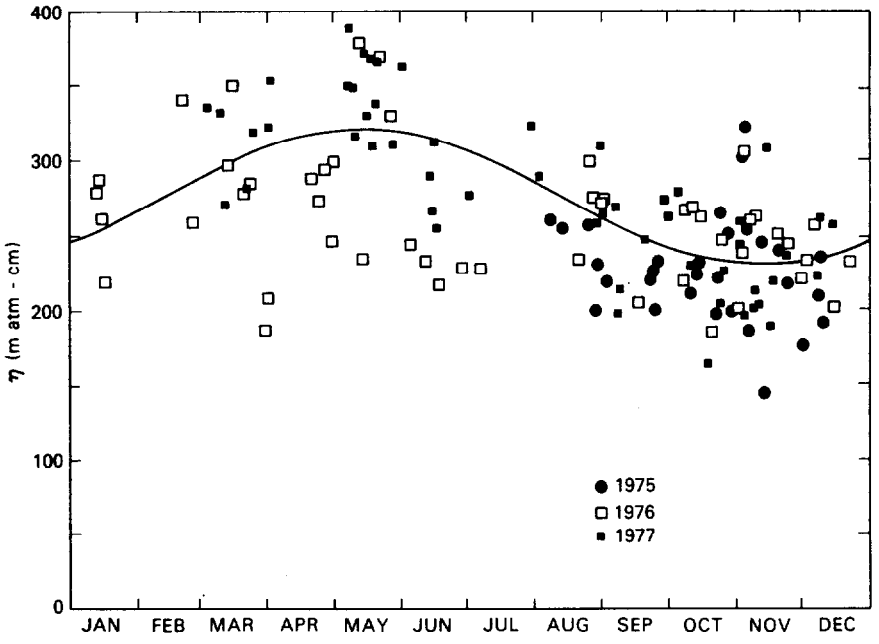

FIG. 5. Daily values of total ozone content inferred from the spectral variation of total optical depth. The solid curve represents a least-squares sinusoidal fit to the data of the form $\eta(x) = 275 + 45 \sin(2\pi x - 0.72)$, where x is the fractional time of year.

Early in July the prevailing winds arrive from a southerly direction, carrying hot humid air from the Gulf of Mexico and the Gulf of Lower California. The aerosol optical depths are typically largest during the "monsoon" months of July and August with a relatively large average for the Ångström turbidity coefficient (see Fig. 4 and Table 2). As discussed by King *et al.* (1978), this is the period in which Junge types of aerosol size distributions are observed (at least for the radius range $0.10 \leqslant r \leqslant 4.0\ \mu$m). Junge types of size distributions also occur in the fall and late spring when the optical depths are relatively large and α is large. Log-normal types of size distributions predominate in the months of May, June, October and November on days with low values of both τ_a and α, and particularly when $\alpha \leqslant 0.0$. Throughout most of the winter months the optical depths are intermediate in magnitude with intermediate values of α and size distributions occur which appear to be combinations of Junge and log-normal distributions (King *et al.*, 1978). It is likely that the aerosol size distribution in the radius range $0.10 \leqslant r \leqslant 4.0\ \mu$m consists of the accumulation and coarse particle modes described by Whitby (1978). Results of the present investigation as well as those of King et al. (1978) suggest that the relative concentration of particles in these two modes varies significantly with time of year.

Peak values of turbidity in the summer months of June, July and August and low values in December and January are frequently reported in the literature (e.g., Flowers *et al.*, 1969; Roosen *et al.*, 1973; Malm *et al.*, 1977; Peterson *et al.*, 1978b). In particular, Flowers *et al.* (1969) demonstrate, based on optical thickness results for 29 U.S. stations, that high turbidities are normally associated with high humidities characteristic of maritime tropical air masses. Low turbidities, on the other hand, were found to be associated with continental polar air masses, air masses which normally occur more often in winter.

Monthly average values of the Ångström turbidity coefficient are also presented in Table 2. The value of α for each individual day was determined by making a linear least-squares fit to $\log\tau_a$ as a function of $\log\lambda$ for the entire wavelength range of the measurements (normally 0.4400–0.8717 μm). The monthly average values are the largest in July and August and the smallest in June, as apparent on examination of Fig. 4. The value of α corresponding to the *median* turbidity measurements of Fig. 2 is 0.65, while the *mean* value of α for the entire data set is 0.46. This mean value corresponds closely to the mean annual value of 0.5 for Poona, India (Rangarajan, 1972), but is quite different than averages of 1.63 for Mauna Loa (Shaw, 1979a), 1.3 for Le Houga, France (Irvine and Peterson, 1970), and −0.13 for Page, Arizona (Malm *et al.*, 1977). Care should be taken in comparing values of α from different investigations since the wavelength intervals used are not always the same. Roosen *et al.* (1973), using predominantly a single wavelength range for a wide range of geographic locations, found that small values of α occur

for desert and semi-arid regions, while large values occur for areas surrounded by vegetation.

Fig. 5 illustrates the inferred ozone content (η) for 133 days between August 1975 and December 1977. These observations include the 40 days previously described by King and Byrne (1976). The large daily variability and seasonal variability which characterizes the measurements of total ozone is readily seen. Worldwide measurements of total ozone content, as summarized by London *et al.*[4], indicate that atmospheric total ozone varies in an approximately sinusoidal manner being well represented by only the first (annual) harmonic at the latitude of Tucson. The solid curve in Fig. 5 thus represents a weighted least-squares fit to a sinusoidal function of the form

$$\eta(x) = \bar{\eta} + A \sin(2\pi x - \phi), \qquad (6)$$

where x is the fractional time of year, and $\bar{\eta}$, A and ϕ are the mean, amplitude and phase of the annual variation, respectively. The resulting curve indicates that the maximum ozone content occurs about 13 May and the minimum occurs about 11 November, with a mean annual value of 275 ± 2 m atm-cm and a seasonal amplitude of 45 ± 2 m atm-cm. Typical uncertainty estimates for the individual ozone data points are 20 m atm-cm as discussed by King and Byrne (1976).

Based on Dobson ozone spectrophotometer observations over a 10-year period, London *et al.*[4] estimated the mean annual value of O_3 at Tucson to be about 290 m atm-cm with a seasonal amplitude of about 30 m atm-cm. This indicates that our estimate for the magnitude of $\eta(x)$ near the seasonal maximum is about the same as Dobson estimates but our annual amplitude is larger, implying lower values of total ozone near the seasonal minimum. These differences may partially be associated with uncertainties in the O_3 absorption coefficients, either in the ultraviolet or visible wavelengths regions, or both. Recent measurements[5] show the O_3 absorption coefficients at selected wavelengths in the Chappuis band to be in good agreement with previous literature values, whereas measurements at two UV wavelengths indicate values approximately 6% smaller than previous values.

The data for most of the individual days illustrated in Fig. 5 show the expected magnitude of daily variability about the sinusoidal regression curve. Only in the case of results for the spring of 1976 are the ozone contents unexpectedly low. Careful examination of the optical depth data during this period indicates that much larger values of η would require an unreasonable wavelength dependence for the aerosol optical depths, a result which could not be explained by any reasonable aerosol size distribution.

5. Summary and conclusions

Results have been presented of the monthly averaged values of total and aerosol optical depths at Tucson, Arizona between August 1975 and December 1977. During this period five of the eight filters in the multi-wavelength solar radiometer were in continuous use and thus results have been presented for these wavelengths only. These filters, whose wavelengths were centered between 0.4400 and 0.8717 μm, were selected to avoid the bands of strong selective absorption by the atmosphere (see Fig. 1 and Table 1). Since careful examination of the entire 133-day data set indicates that the probability distribution of aerosol optical depths is nearly log-normally distributed, geometric means and logarithmic standard deviations of the total and aerosol optical depths were computed for each month and wavelength. These results, which have been presented in Figs. 3 and 4 and in Table 2, indicate that the aerosol optical depth (τ_a) obtains a maximum in July and August with a secondary maximum in April and May. The minimum values of τ_a occur in June and in December and January (see Fig. 4). The relatively large turbidities in July and August are at least partly associated with the hot humid air mass flowing into much of Arizona from a southerly direction. The low turbidities in June occur prior to the "monsoon" season and the prevailing winds are from the west, carrying hot dry air.

As seen upon examination of Fig. 4 and Table 2, the Ångström turbidity coefficient (α) is largest during the summer and early fall and lowest in June. The largest values of α are normally associated with high turbidities, while low values of α are associated with low turbidities. Fig. 2, which indicates the total percentage of days with turbidities below a certain level, also shows the general correlation of high turbidities with high values of α. The median aerosol optical depth for the entire data set decreases with wavelength from 0.0508 (λ = 0.4400 μm) to 0.0306 (λ = 0.8717 μm) with an Ångström turbidity coefficient α = 0.65.

The values of total ozone content (η) presented here (see Fig. 5) indicate the presence of an overall seasonal cycle with peak values in early May. These ozone results are similar to other measurements obtained with Dobson ozone spectrophotometers for similar latitudes, both in average seasonal characteristics (London *et al.*)[4] and in the magnitudes of the daily fluctuations. The results presented here have an annual mean which is ~15 m atm-cm lower

[4] London, J., R. D. Bojkov, S. Oltmans and J. I. Kelley, 1976: *Atlas of the Global Distribution of Total Ozone July 1957–June 1967*. NCAR Tech. Note 113+STR, 276 pp. [NTIS PB258882/0].

[5] Penny, C. M., 1979: Study of temperature dependence of the Chappuis band absorption of ozone. NASA CR-158977, General Electric Company, Schenectady, NY, 22 pp.

than Dobson results and a seasonal amplitude which is ~15 m atm-cm higher than Dobson results. These differences may be associated with uncertainties in the O_3 absorption coefficients.

Acknowledgments. The authors are grateful to R. L. Peck of the Department of Electrical Engineering at the University of Arizona for maintaining the solar radiometer and to T. Ashbaugh for data processing assistance. The research reported in this article has been supported by the National Science Foundation under Grants DES75-15551, ATM75-15551-A01 and ATM77-24493 and the Office of Naval Research under Grant N00014-76-C-0438.

REFERENCES

Ackerman, M., 1971: Ultraviolet solar radiation related to mesospheric processes. *Mesospheric Models and Related Experiments*, G. Fiocco, Ed., D. Reidel, 149–159.

Ångström, A., 1929: On the atmospheric transmission of sun radiation and on dust in the air. *Geogr. Ann.*, **11**, 156–166.

Bevington, P. R., 1969: *Data Reduction and Error Analysis for the Physical Sciences*. McGraw-Hill, 336 pp.

Carlson, T. N., and R. S. Caverly, 1977: Radiative characteristics of Saharan dust at solar wavelengths. *J. Geophys. Res.*, **82**, 3141–3152.

Chu, W. P., and M. P. McCormick, 1979: Inversion of stratospheric aerosol and gaseous constituents from spacecraft solar extinction data in the 0.38–1.0 μm wavelength region. *Appl. Opt.*, **18**, 1404–1413.

Flowers, E. C., R. A. McCormick and K. R. Kurfis, 1969: Atmospheric turbidity over the United States, 1961–1966. *J. Appl. Meteor.*, **8**, 955–962.

Fraser, R. S., 1975: Degree of interdependence among atmospheric optical thicknesses in spectral bands between 0.36–2.4 μm. *J. Appl. Meteor.*, **14**, 1187–1196.

Golovachev, V. P., V. Y. Pavlov, G. A. Studenina and Y. A. Teyfel, 1972: Atmospheric transparency and the relationships between optical variables in the ultraviolet. *Izv. Atmos. Oceanic Phys.*, **8**, 508–510.

Gucker, F. T., S. Basu, A. A. Pulido and G. Chiu, 1969: Intensity and polarization of light scattered by some permanent gases and vapors. *J. Chem. Phys.*, **50**, 2526–2535.

Hoyt, D. V., 1977: A redetermination of the Rayleigh optical depth and its application to selected solar radiation problems. *J. Appl. Meteor.*, **16**, 432–436.

Irvine, W. M., and F. W. Peterson, 1970: Observations of atmospheric extinction from 0.315 to 1.06 microns. *J. Atmos. Sci.*, **27**, 62–69.

King, M. D., and D. M. Byrne, 1976: A method for inferring total ozone content from the spectral variation of total optical depth obtained with a solar radiometer. *J. Atmos. Sci.*, **33**, 2242–2251.

——, ——, B. M. Herman and J. A. Reagan, 1978: Aerosol size distributions obtained by inversion of spectral optical depth measurements. *J. Atmos. Sci.*, **35**, 2153–2167.

Koepke, P., and H. Quenzel, 1978: Water vapor: Spectral transmission at wavelengths between 0.7 μm and 1 μm. *Appl. Opt.*, **17**, 2114–2118.

Malm, W. C., and E. G. Walther, 1979: Reexamination of turbidity measurements near Page, Arizona, and Navajo generating station. *J. Appl. Meteor.*, **18**, 953–955.

——, —— and R. A. Cudney, 1977: The effects of water vapor, ozone and aerosol on atmospheric turbidity. *J. Appl. Meteor.*, **16**, 268–274.

Minnaert, M., G. Mulders and J. Houtgast, 1940: *Photometric Atlas of the Solar Spectrum from λ3612 to λ8771*. Sterrewacht Sonnenborgh, Utrecht.

Moore, C. E., M. G. J. Minnaert and J. Houtgast, 1966: *The Solar Spectrum 2935 Å to 8770 Å; Second Revision of Rowland's Preliminary Table of Solar Spectrum Wavelengths*. Nat. Bur. Stand. Monogr. No. 61, U.S. Govt. Printing Office, Washington, DC, 349 pp.

Peterson, J. T., E. C. Flowers and J. H. Rudisill III, 1978a: Atmospheric turbidity across the Los Angeles basin. *J. Appl. Meteor.*, **17**, 428–435.

——, —— and ——, 1978b: Urban-rural solar radiation and atmospheric turbidity measurements in the Los Angeles basin. *J. Appl. Meteor.*, **17**, 1595–1609.

Quenzel, H., 1970: Determination of size distribution of atmospheric aerosol particles from spectral solar radiation measurements. *J. Geophys. Res.*, **75**, 2915–2921.

Rangarajan, S., 1972: Wavelength exponent for haze scattering in the tropics as determined by photoelectric photometers. *Tellus*, **24**, 56–64.

Roosen, R. G., R. J. Angione and C. H. Klemcke, 1973: Worldwide variations in atmospheric transmission: 1. Baseline results from Smithsonian observations. *Bull. Amer. Meteor. Soc.*, **54**, 307–316.

Rozenberg, G. V., 1966: *Twilight: A Study in Atmospheric Optics* (English translation). Plenum Press, 358 pp.

Russell, P. B., and G. E. Shaw, 1975: Comments on "The precision and accuracy of Volz sunphotometry." *J. Appl. Meteor.*, **14**, 1206–1209.

Shaw, G. E., 1976: Error analysis of multi-wavelength sun photometry. *Pure Appl. Geophys.*, **114**, 1–14.

——, 1979a: Aerosols at Mauna Loa: Optical properties. *J. Atmos. Sci.*, **36**, 862–869.

——, 1979b: Atmospheric ozone: Determination by Chappuis-band absorption. *J. Appl. Meteor.*, **18**, 1335–1339.

——, J. A. Reagan and B. M. Herman, 1973: Investigations of atmospheric extinction using direct solar radiation measurements made with a multiple wavelength radiometer. *J. Appl. Meteor.*, **12**, 374–380.

Whitby, K. T., 1978: The physical characteristics of sulfur aerosols. *Atmos. Environ.*, **12**, 135–159.

Yamamoto, G., and M. Tanaka, 1969: Determination of aerosol size distribution from spectral attenuation measurements. *Appl. Opt.*, **8**, 447–453.